Exp Brain Res (2011) 209:35–50
DOI 10.1007/s00221-010-2514-x

RESEARCH ARTICLE

# Unconstrained three-dimensional reaching in Rhesus monkeys

**Devin L. Jindrich · Gregoire Courtine · James J. Liu · Heather L. McKay · Rod Moseanko · Timothy J. Bernot · Roland R. Roy · Hui Zhong · Mark H. Tuszynski · V. Reggie Edgerton**

Received: 25 May 2010 / Accepted: 29 November 2010 / Published online: 19 December 2010


**Abstract** To better understand normative behavior for quantitative evaluation of motor recovery after injury, we studied arm movements by non-injured Rhesus monkeys during a food-retrieval task. While seated, monkeys reached, grasped, and retrieved food items. We recorded three-dimensional kinematics and muscle activity, and used inverse dynamics to calculate joint moments due to gravity, segmental interactions, and to the muscles and tissues of the arm. Endpoint paths showed curvature in three dimensions, suggesting that maintaining straight paths was not an important constraint. Joint moments were dominated by gravity. Generalized muscle and interaction moments were less than half of the gravitational moments. The relationships between shoulder and elbow resultant moments were linear during both reach and retrieval. Although both reach and retrieval required elbow flexor moments, an elbow extensor (triceps brachii) was active during both phases. Antagonistic muscles of both the elbow and hand were co-activated during reach and retrieval. Joint behavior could be described by lumped-parameter models analogous to torsional springs at the joints. Minor alterations to joint quasi-stiffness properties, aided by interaction moments, result in reciprocal movements that evolve under the influence of gravity. The strategies identified in monkeys to reach, grasp, and retrieve items will allow the quantification of prehension during recovery after a spinal cord injury and the effectiveness of therapeutic interventions.

**Keywords** Upper limb · Prehension · Multi-joint · Reach-to-grasp · Kinematics · Dynamics · Muscle · Electromyography · EMG

D. L. Jindrich (✉)
School of Life Sciences, Center for Adaptive Neural Systems,
427 E. Tyler Mall; LSE 216, Arizona State University,
Tempe, AZ 85287-4501, USA
e-mail: devin.jindrich@asu.edu

G. Courtine
Experimental Neurorehabilitation,
Department of Neurology, Universitat Zurich,
August Forel-Strasse 7, 8008 Zurich, Switzerland
e-mail: gregoire.courtine@bli.uzh.ch

J. J. Liu · R. R. Roy · H. Zhong · V. Reggie Edgerton
Department of Integrative Biology and Physiology,
University of California, Los Angeles, CA, USA

H. L. McKay · R. Moseanko · T. J. Bernot
California National Primate Research Center,
University of California, Davis, CA, USA

M. H. Tuszynski
Department of Neurosciences,
University of California,
San Diego, La Jolla, CA, USA

M. H. Tuszynski
Veterans Administration Medical Center, San Diego, CA, USA

## Introduction

The Rhesus monkey is an important animal model for evaluating the potential of selected therapies for neuromotor disorders such as spinal cord injury (Courtine et al. 2007). Monkeys also are extensively used to develop engineered systems such as brain–machine interfaces for arm control (Hochberg et al. 2006; Jackson et al. 2006; Kim et al. 2007) as well as determining the fundamental properties of the neural control of movement. Consequently, understanding arm movements can facilitate neurobiological, therapeutic, and engineering approaches to functional restoration after an injury.

Limb dynamics reflect the complex interactions among segments, variable external forces, and redundant degrees of freedom (DOF) (Bernstein 1967). Specific coordination rules could facilitate the selection of movement patterns. Planar point-to-point movements in humans are commonly achieved using nearly straight hand paths (Morasso 1981; Soechting and Lacquaniti 1981; Shemmell et al. 2007; Yamasaki et al. 2008), and neuromotor deficits can result in increased movement curvature (Bastian et al. 1996). Constraints on limb endpoint paths could reduce the number of available trajectories and facilitate movement selection and planning. During many movements, shoulder and elbow joint velocities and moments are linearly correlated (Soechting and Lacquaniti 1981; Lacquaniti and Soechting 1982; Gottlieb et al. 1996a, b; Gottlieb et al. 1997). Linear coupling could reflect an organizing principle used by the nervous system to simplify control (Gottlieb et al. 1996b; Graham et al. 2003; Shemmell et al. 2007). Structuring activity also could simplify muscle recruitment patterns during movement. For example, muscle activity underlying planar arm movements is characterized by triphasic EMG burst patterns that can be scaled to achieve different movements (Hannaford and Stark 1985; Gottlieb et al. 1989; Gottlieb 1998).

Kinematic, dynamic, and neuromuscular movement strategies have primarily been studied in planar arm movements to simplify their dynamics (Hollerbach and Flash 1982; Shadmehr and Mussa-Ivaldi 1994; Gomi and Kawato 1996; Gribble and Ostry 1999; Sainburg et al. 1999; Galloway and Koshland 2002; Franklin et al. 2003). Natural movements, however, are three-dimensional, unconstrained, and occur in a gravitational field. Three-dimensional, multi-joint movements differ from planar movements in several respects. Although both planar and three-dimensional movements are kinematically redundant (many possible movements can lead to the same endpoint position), three-dimensional movements require control in a larger parameter space (Soechting et al. 1995). Moreover, three-dimensional movement dynamics of segmented systems such as the arm are complex because generating joint moments in one direction can result in movements in other directions and at other joints (Hirashima et al. 2007b). Movements that are mechanically constrained to be planar may not need to account for the interactions that can affect multi-joint systems in three dimensions.

Natural joint movements also must account for the effects of gravity (Fisk et al. 1993; Pozzo et al. 1998; Papaxanthis et al. 2005; Gentili et al. 2007). Although the contribution of gravity to human arm dynamics has been discounted (Hollerbach and Flash 1982), gravity could potentially act to reduce required muscle forces, increase muscle forces, or even change the muscle activity patterns required depending on the desired movement (Virji-Babul et al. 1994). The potential for gravity to substantially alter the neural control of movement presents questions about whether the principles used to organize constrained, planar movements apply to unconstrained, multi-joint, three-dimensional arm movements.

The goal of this study was to investigate the strategies used for reaching movements by seated Rhesus monkeys. Given that the kinematics and dynamics of prehension are similar in monkeys and humans (Scott et al. 1997; Roy et al. 2000, 2002, 2006; Christel and Billard 2002; Mason et al. 2004), characterization of monkey prehension is likely to provide a better understanding of three-dimensional arm movement in primates, and in further developing a valuable animal model of neuromotor injury or disease.

We focused on four specific questions. First, we sought to determine whether monkeys constrain endpoint position to straight paths during natural movements. The observation of straight endpoint paths would support the hypothesis that monkeys regulate endpoint trajectories during reaching. Second, we sought to determine whether moments due to gravity are a substantial contributor to joint moments (relative to the moments necessary for segmental accelerations and moments due to interactions among segments). If gravitational moments contribute substantially to total joint moments, then assessing interactions with gravity may be useful for evaluating arm function. Third, we tested whether a linear relationship between shoulder and elbow joint moments is observed during three-dimensional reaching. Linear joint moment relationships could simplify the control of multi-joint movements. Fourth, we sought to determine whether joint behavior during unconstrained movements could be described using a lumped-parameter model.

We found that gravity made a substantial contribution to total joint moments, and joint behavior could be described by lumped-parameter quasi-stiffness models. These results were consistent with the hypothesis that during unconstrained three-dimensional movements, joint muscle and interaction moments are organized to modulate moments due to gravity, and that endpoint paths and joint moment coupling emerged from these interactions. These results also suggest that analysis of movement dynamics may be useful for evaluating and understanding recovery of coordination after injury.

## Materials and methods

We studied 5 Rhesus monkeys (Macaca mulatta) with a mean mass of 12 ± 2 kg. All surgical and experimental procedures in these experiments were carried out using the principles outlined by the Laboratory Animal Care (National Institutes of Health Publication 85–23, revised

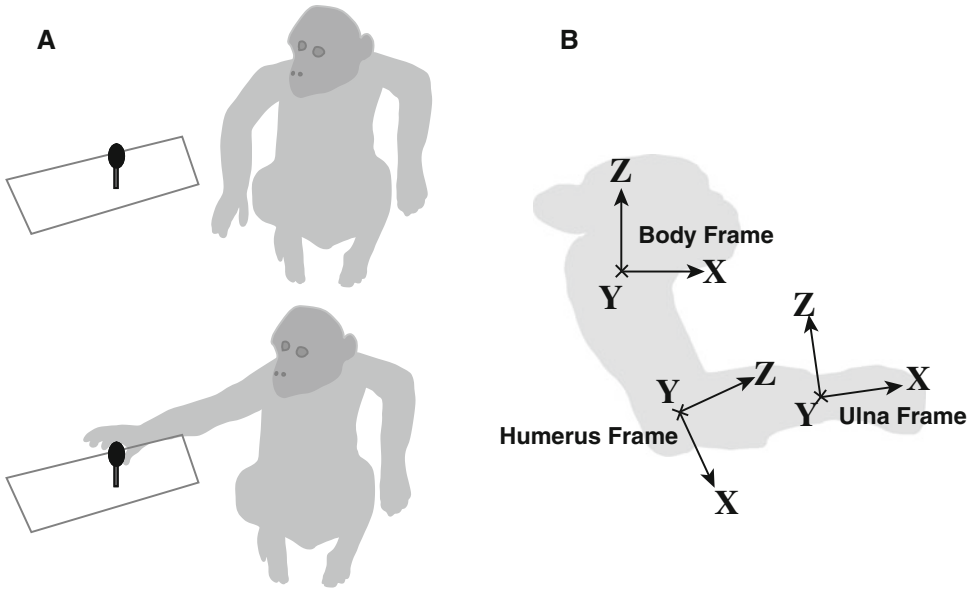


**Fig. 1** Experimental setup and angle conventions used. **a** The monkey sat in a chair and reached for a grape positioned 31 ± 2 cm from the shoulder. **b** Angle conventions used to describe rotations of the arm. Coordinate frames were located approximately at joint centers, with *X*-axes aligned with the segment proximal to the joint

1996) and were approved by the Institutional Animal Care and Use Committee (IACUC). The monkeys were trained to sit and retrieve food items (grapes) impaled on a metal post 28 cm anterior and 33 cm lateral to the shoulder (Fig. 1a). Similar to previous studies (Wenger et al. 1999), monkey head position was constrained by a collar, which also prevented trunk movements (average maximum shoulder displacement in any direction was 1.2 ± 0.7 cm). Prior to moving, the monkeys held their arm with the humerus approximately in the coronal plane and the forearm in approximately the sagittal plane and were restrained from reaching using an acrylic barrier. When the barrier was removed, the monkeys were free to reach, manipulate, and retrieve the grape to their mouths. The monkeys were presented with 10 grapes in succession, and the acrylic barrier was placed between the arm and the grape with each presentation. We analyzed a total of 48 trials from the 5 monkeys.

The three-dimensional positions of five skin markers attached to the arm were measured at 100 Hz using a four-camera motion-tracking system (SIMI Reality Motion Systems GmbH, Unterschleissheim, Germany). Skin markers were placed on the shoulder directly lateral to the glenohumeral joint, the lateral epicondyle of the humerus, the radial and ulnar styloid processes, and the dorsal aspect of the first metacarpophalangeal joint. Kinematic data from joint markers were filtered using a fourth-order low-pass Butterworth filter with a cut-off frequency of 7 Hz, following procedures used for analyzing human arm movement data at similar frequencies (Dounskaia et al. 2005).

Endpoint kinematics were estimated using three-dimensional kinematic data from the ulnar styloid process. Radius of curvature was calculated from endpoint kinematics and its derivatives using previously reported equations (Eq. 1 in Schaal and Sternad 2001). We modeled the arm as a chain of rigid segments connected by frictionless rotational joints. The shoulder was modeled as rotating in three dimensions: in flexion/extension, abduction/adduction, and humeral rotation. The body reference frame was set so that the *Z*-axis was vertical, the *X*-axis was in the parasagittal (*X*–*Z*) plane (0° horizontal), and the positive *Y*-axis projected medially (Fig. 1b). The orientation of the humerus was expressed relative to the body using Euler angles in the order *Z* then *Y*, to align the *X*-axis along the long axis of the humerus. Rotation about the *Z*-axis approximates flexion/extension (positive values denote flexion) and rotation about the *Y*-axis approximates abduction/adduction of the shoulder joint relative to the body (positive values denote adduction from 0° where the upper arm lies in the horizontal, or transverse, plane), although the correspondence between Euler angles and common clinical definitions of rotations is not exact (Wu et al. 2002, 2005). Finally, rotation about the *X*-axis describes humeral rotation as measured by the rotation of the ulna around the long axis of the humerus (negative values denote internal rotation from 0° where the forearm lies in the coronal plane). Forearm rotation (pronation/supination) is unlikely to substantially affect humeral rotation measured using the ulna, since it is characterized by rotation of the radius about the ulna and small ulnar translation (Nakamura et al. 1999). Each successive segment was related to the proximal segment using Euler angles in the order *Z*, *Y*, and *X*. For joints distal to the shoulder, *Z*-rotation corresponds to abduction/adduction of the distal segment (assumed to be zero for the elbow), *Y*-rotation corresponds to flexion–extension (negative values denote flexion from the fully extended position at 0°), and *X*-rotation corresponds to rotation of the distal segment

about its long axis. Flexion/extension of the elbow was measured as the movement of the ulna relative to the humerus. Pronation/supination of the forearm was measured as the rotation of the radial styloid process about the ulna. For simplicity, the wrist was considered as fixed in the neutral position for dynamics calculations.

Joint Euler angles were calculated for each sampled time point, then differentiated to yield velocity and differentiated again to yield acceleration using a fourth-order difference equation. Segment inertias were calculated based on the body mass of the monkeys and the relationships of Table 8 in Cheng and Scott (2000). Using the kinematics, segment masses, and inertias, joint moments were calculated using an iterative Newton–Euler algorithm (Craig 1989; see "Appendix"). The segmental moment ($M_{SEG}$; the moment that causes segment rotation) was decomposed into components following the equation:

$$M_{SEG} = M_{GM} + M_{GRAV} + M_{INT} \quad (1)$$

where $M_{GM}$ (Generalized Muscle Moment) is the moment due to muscles and other tissues at the joints, $M_{GRAV}$ is the moment due to gravity, and $M_{INT}$ is the moment due to segment interactions.

Reach and retrieval phases of the movement were distinguished by visually identifying the time point when any finger first touched the grape, a time point that was distinct and specific for all trials. Because the monkeys typically did not pause to grasp the grape resulting in continuous joint movements during grasping and retrieval, both the grasping and retrieval periods of movement were included in the retrieval phase.

The moment impulse for each DOF during the reach and retrieval phases was calculated by integrating joint moment with respect to time. Work was calculated by integrating joint moment with respect to angle. The degree of linear coupling between the shoulder and elbow was determined by calculating linear merit ($\Phi_{LM}$) values from shoulder versus elbow resultant joint moment magnitudes (Gottlieb et al. 1997; Eq. *A2*). The linear merit is a measure of how much of the variance of the shoulder versus elbow relationship a linear fit can account for, independent of the slope of the line. A straight line would have a $\Phi_{LM}$ value of 1 and a circle a value of 0.

EMG electrodes were chronically implanted intramuscularly as described previously (Courtine et al. 2005a, b). Briefly, skin incisions were made over the bellies of the biceps brachii (biceps), triceps brachii (triceps), extensor digitorum communis (EDC), flexor digitorum superficialis (FDS), pronator teres (pronator) and the thenar eminence (to access the flexor pollicis brevis (pollicis). These muscles were selected to allow for measurement from arm DOFs important for prehension and locomotion, with an emphasis on distal muscles that are disrupted by C6–C7 hemisection lesions used in primate models of SCI (Brock et al. 2010; Rosenzweig et al. 2010). Wires were routed to the incision sites from a percutaneous connector on the upper mid-back. EMG electrodes were implanted in the right medial mid-belly of the medial head of the triceps, lateral mid-belly of the long head of the biceps, lateral mid-belly of the EDC, the mid-belly of the pronator, and in the right and left lateral mid-belly of the FDS and mid-belly of the pollicis. The EMG wires were coiled near each implant site to provide stress relief. Back stimulation was used to verify the proper placement of the electrodes in each muscle, and electrode placement was verified in a terminal experiment at the end of the study. One monkey (31334) rejected the EMG implants, and consequently no data were collected or included in the EMG analyses. In monkey 30568, the pronator was not implanted.

EMG signals were recorded simultaneously with kinematics at 2 kHz and saved for post-processing. EMG signals from each muscle were baseline-corrected and filtered using a Butterworth bandpass filter with a low cutoff of 30 Hz and high cutoff of 1 kHz. It was not possible to measure EMG during maximum voluntary contractions during these experiments. Consequently, to enable comparisons of the EMG signals among monkeys, the signals were normalized to the mean EMG burst amplitudes during quadrupedal locomotion at 0.45 m $s^{-1}$. EMG during locomotion was used for normalization because locomotion is characterized by consistent, repeatable patterns of muscle activity that contrast with the more variable muscle activity observed during unloaded arm movements, and normalization to locomotion will allow direct comparisons of EMG measurements to concurrent studies of locomotion in these monkeys (Courtine et al. 2005a). Bursting activity was identified as EMG exceeding 4 times the standard deviation of baseline noise for each channel. The 90th percentile of the amplitude distribution was identified to approximate the maximum burst amplitude for bursts present during 10 s of consistent locomotion. EMG recordings from each muscle during food retrieval trials then were normalized to the maximum burst amplitude of the same muscle during locomotion.

All calculations were performed using custom analysis routines written in MATLAB (The Math Works, Inc., Natick, MA, USA). Calculated values were averaged within each monkey, and then averaged across monkeys. Reported values are mean ± standard deviation across monkeys unless otherwise indicated. Statistical comparisons reflect results of repeated-measures ANOVA, with individual monkey as the repeated variable. Statistical tests were performed using JMP 4.0.2 (SAS Institute, Inc.), and comparisons were considered significant at $P < 0.05$.

## Results

The average trial movement time was 2,120 ± 830 ms. Reaching movements were a shorter distance and executed more rapidly than retrieval movements ($P < 0.001$): the average duration was 620 ± 290 ms (29% of the trial) for reach and 1,500 ± 620 ms (71% of the trial) for retrieval. The wrist path length was 18 ± 6 cm for reach, 29 ± 6 cm for retrieval, and 47 ± 11 cm for the entire movement.

Although individual monkeys showed differences in movement magnitude, the basic movement patterns were shared by a majority (4/5) of the monkeys (Fig. 2a–c). Reaching involved shoulder abduction and external rotation, and elbow extension. Both shoulder and elbow movements continued after touching the food item during the manipulation and retrieval period of movement. During retrieval, shoulder adduction and elbow flexion movements were opposite of the movements during reach, although elbow flexion and forearm supination exceeded that during reach (Table 1).

The nearly opposite movements during reach and retrieval did not reflect a qualitative shift in the direction of muscle moments, but instead a shift in the balance among $M_{GM}$, $M_{INT}$, and $M_{GRAV}$. The shoulder generated abductor $M_{GM}$ and the elbow flexor $M_{GM}$ throughout both reach and retrieval (Fig. 3a, e). During reach, shoulder abductor $M_{GM}$ was greater than adductor $M_{GRAV}$ and $M_{INT}$, resulting in abduction $M_{SEG}$ (Fig. 3a–d). At the elbow, flexor $M_{GM}$ was less than extensor $M_{GRAV}$ and $M_{INT}$, resulting in extension $M_{SEG}$ (Fig. 3e–h). During retrieval, shoulder abductor $M_{GM}$ decreased. Although $M_{INT}$ at the shoulder switched from being adductor to abductor, $M_{GM}$ and $M_{INT}$ were still less

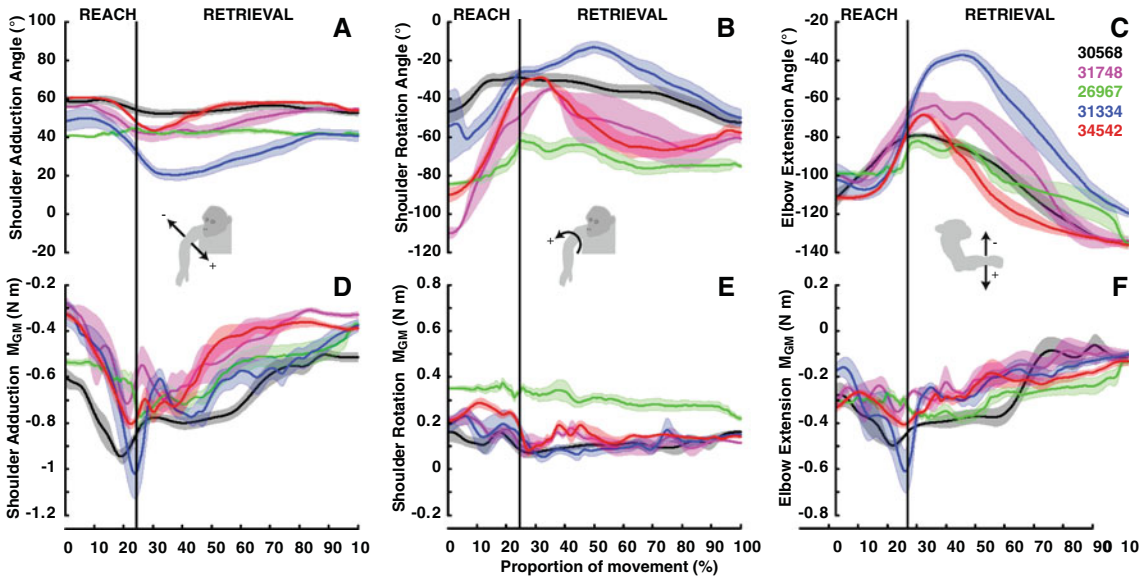


**Fig. 2** Movements and generalized muscle moments for primary shoulder and elbow degrees of freedom. Data from all trials were normalized in time to the mean duration of reach and retrieval phases of motion across all trials. To illustrate the degree of variability in movement strategies used by different monkeys, data for each monkey were averaged and displayed. *Shaded* areas indicate standard errors across individual trials made by each monkey. Colors distinguish averages for each monkey. Major *vertical line* is target touch. **a–c** Reaching involved shoulder abduction, external rotation, and elbow extension. For shoulder *Y* (adduction) angles, a zero angle would indicate that the humerus was horizontal. For shoulder *X* (rotation), a zero value would indicate that the elbow rotation axis is horizontal. For elbow *Y* (extension), a zero value would indicate full extension. Retrieval involved shoulder adduction and elbow flexion, with some degree of internal rotation of the shoulder. **d–f** Generalized muscle moments reflect the importance of resisting gravity for this three-dimensional movement. Negative generalized muscle moments ($M_{GM}$) at the shoulder and elbow are abductor and flexor, respectively, indicating that muscles and tissues of the arm acted to resist gravity during both the reach and retrieval phases of movement

**Table 1** Angular excursions for arm degrees of freedom

| | Reach | Retrieval | *P* |
|---|---|---|---|
| Shoulder flexion/extension excursion (°) | 26 ± 11 | 27 ± 13 | 0.87 |
| Shoulder abduction/adduction excursion (°) | 16 ± 7 | 21 ± 8 | 0.10 |
| Upper arm rotation excursion (°) | 46 ± 20 | 40 ± 12 | 0.14 |
| Elbow flexion/extension excursion (°) | 41 ± 13 | 77 ± 11 | <0.0001 |
| Forearm pronation/supination excursion (°) | 42 ± 24 | 89 ± 16 | <0.0001 |

*P* values indicate reach versus retrieval ANOVA comparison

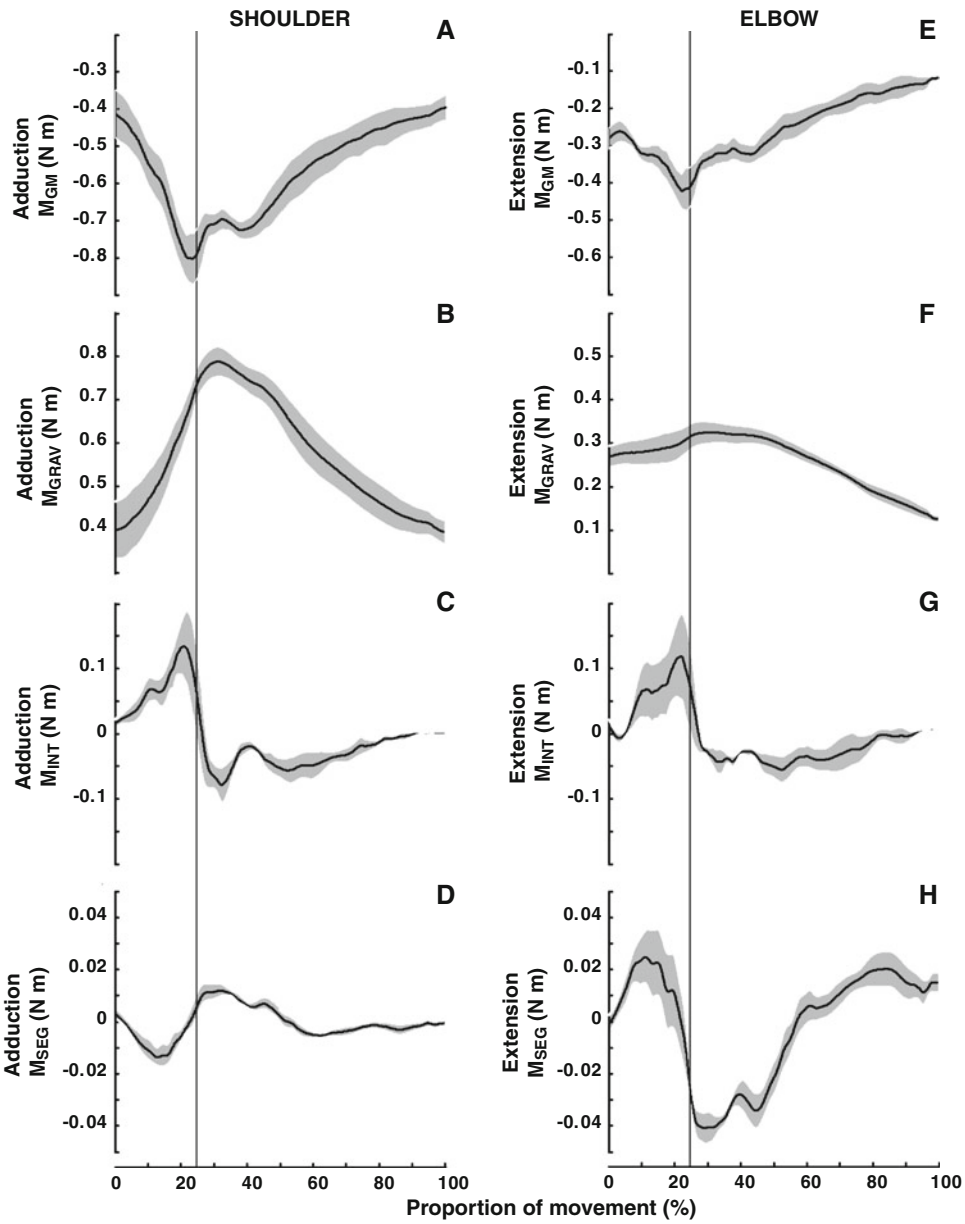


**Fig. 3** Average time series of components of the joint moment for the shoulder (**a**–**d**) and elbow (**e**–**h**). Data were normalized in time to the mean duration of reach and retrieval phases of motion across all trials. Resulting normalized time series were averaged across all trials for each monkey as in Fig. 2, and then averaged across all 5 monkeys. *Shaded areas* represent standard errors of the mean at each phase of the motion

than $M_{GRAV}$, resulting in shoulder adduction $M_{SEG}$. As at the shoulder, during retrieval elbow $M_{INT}$ switched to the same direction as $M_{GM}$. Although elbow $M_{GM}$ also decreased during retrieval, $M_{GM}$ and $M_{INT}$ together were larger than $M_{GRAV}$, resulting in elbow flexion $M_{SEG}$.

## Monkeys did not use straight endpoint trajectories

Monkeys did not use straight endpoint paths when executing three-dimensional reaching movements. Endpoint paths were curved in both the horizontal and parasagittal planes (Fig. 4a). During reach, shoulder abduction and forearm rotation both contributed to endpoint paths that were concave with respect to the elbow. During retrieval, shoulder adduction flattened the curvature due to forearm rotation, ultimately resulting in curvature convex to the elbow at the end. Maximum radius of curvature ($r_{max}$, the maximum value of $r$ over the entire movement—i.e., where it is most straight) occurred before the mid-point of reach (Fig. 4b). Even the most straight instantaneous segments, however, were still substantially curved. Since 3 of 96 values for $r_{max}$ were clearly outliers (values 20–60 times the standard deviation of the remaining 93 values), we report median radius of curvature and excluded these trials from the averages and Fig. 4b. The median $r_{max}$ averaged across monkeys was $26 \pm 16$ and $62 \pm 39$ cm or $1.5 \pm 0.7$ and $2.3 \pm 1.4$ times the total wrist path length during reach and retrieval, respectively. Reach and retrieval $r_{max}$ values were not significantly different due to the high variance in retrieval values (range from 23 to

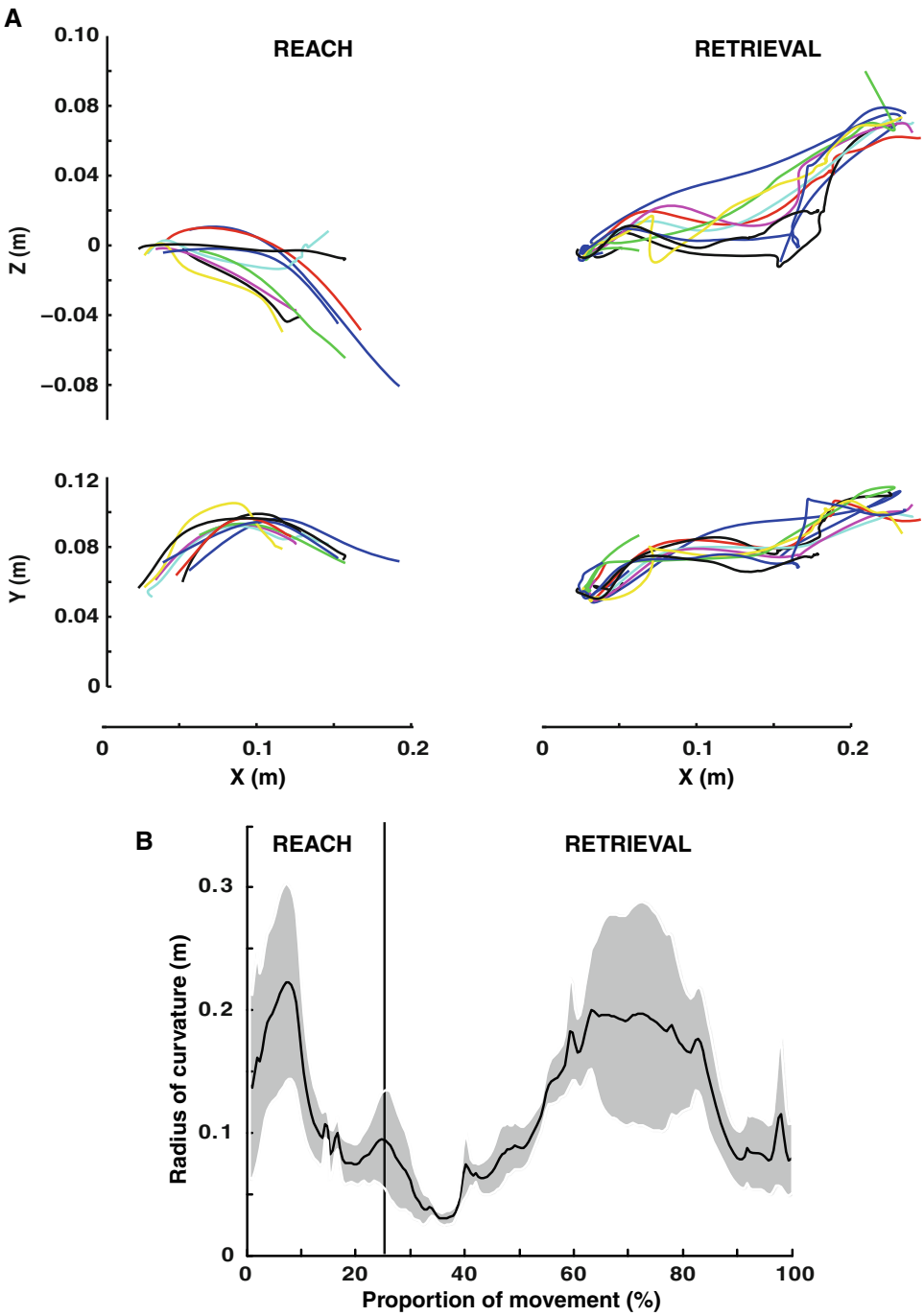


**Fig. 4** Wrist path curvature during reach and retrieval movements. **a** Wrist paths for nine reaching trials from one monkey (34542). Each line represents a separate trial. *Top graphs* show projection of three-dimensional movements onto a plane approximately parasagittal; *bottom graphs* show projections onto the horizontal plane. **b** Instantaneous radius of curvature averaged across all 5 monkeys studied. Radius of curvature time series were scaled in time during reach and retrieval phases, averaged within each monkey, and then averaged across all monkeys. *Shaded areas* indicate point-wise standard errors of the mean across all monkeys. Three outliers were excluded from the analysis (see text)

104 cm). The average forearm length was 17 ± 1 cm; $r_{max}$ was ±1.7 or 4.0 ± 2.5 times forearm length during reach and retrieval, respectively.

## Gravitational moments were the largest contributors to net joint moments

$M_{GRAV}$ was the largest component of the joint moments during both reach and retrieval (with the exception of shoulder flexion/extension, which are de-coupled from gravity; Fig. 5). By integrating the absolute value of each component of the total moment with respect to time, we calculated the absolute moment impulse for each joint DOF, which expresses the total moments produced irrespective of whether or not they were associated with movement. By summing the absolute value of the instantaneous work for the reach and retrieval periods, we determined the total work associated with movement. $M_{GRAV}$ accounted for over 68% of the total absolute moment impulses (Fig. 5a) and 58% of the total work

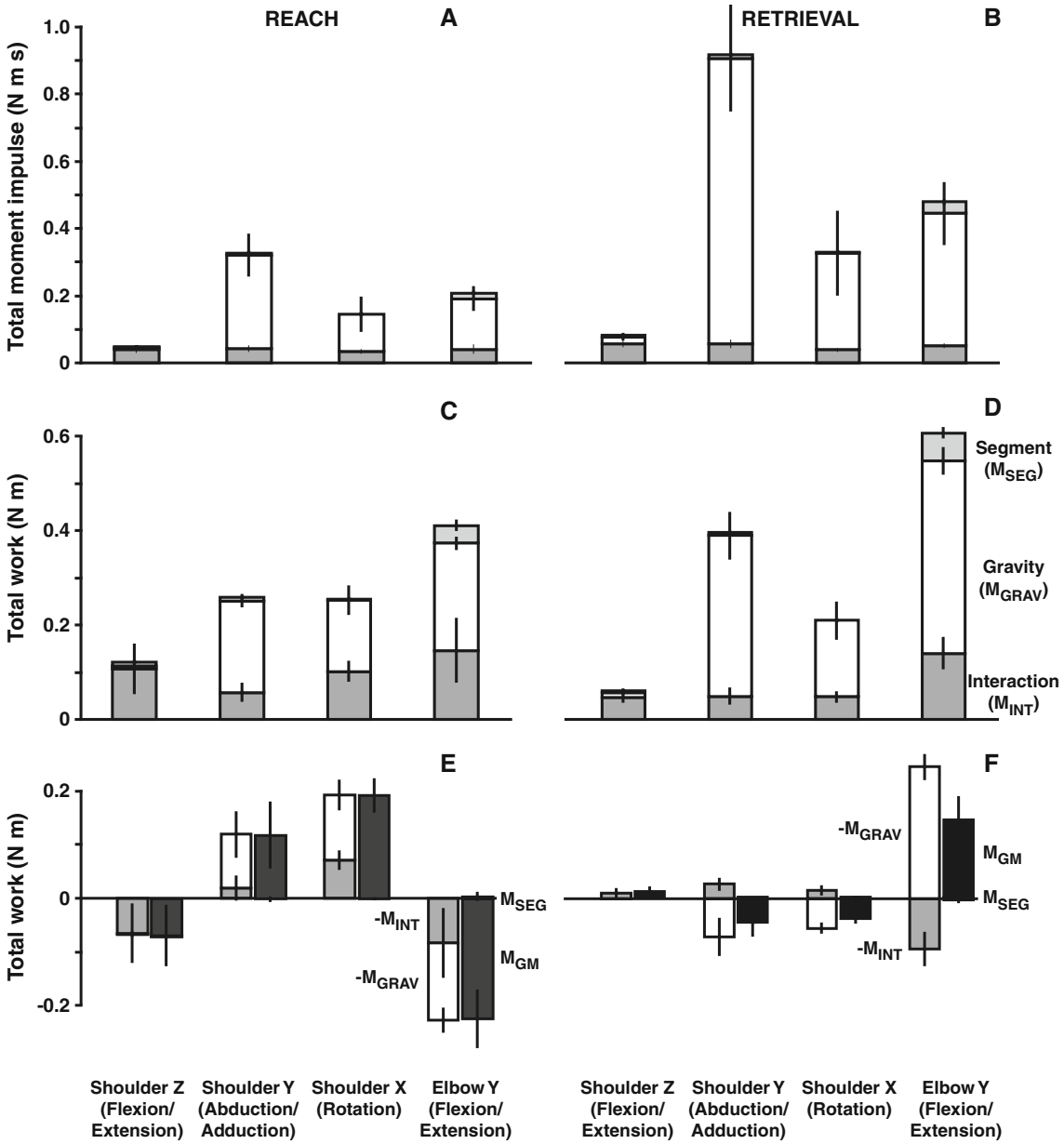


**Fig. 5** Contributions of moment components to total moments during movement. **a**, **b** Total absolute moment impulses for primary shoulder and elbow degrees of freedom. Moment impulse was calculated by integrating the absolute value of each component of moment with respect to time. **c**, **d** Total absolute work was calculated as the sum of the absolute value of instantaneous work for each component of the muscle moment. Consequently, these values represent the maximum amount of impulse or work that the moment component could contribute to the total impulse or work. **e**, **f** Total work by moment components averaged across all monkeys. $M_{INT}$ and $M_{GRAV}$ have been negated to facilitate comparison to $M_{GM}$ and represent the energy to/from muscles and tissues to other segments and gravitational potential energy. $M_{SEG}$ was small for all degrees of freedom. During reach, $M_{INT}$ and $M_{GRAV}$ were of the same sign, whereas during retrieval $M_{INT}$ moments opposed $M_{GRAV}$

(Fig. 5c) during reach for shoulder abduction, rotation, and elbow flexion. During retrieval, $M_{GRAV}$ was an even greater proportion of the total, accounting for over 80% of the absolute moment impulses (Fig. 5b) and 68% of the total work (Fig. 5d). Moment impulses and work due to gravity were significantly larger than both $M_{INT}$ and $M_{SEG}$ during both reach and retrieval for shoulder abduction, rotation, and elbow flexion ($P < 0.001$). Moments in the *Z*-direction (flexion/extension) at the shoulder were small since the *Z*-axis was nearly vertical and consequently moments were not necessary to resist gravity.

$M_{INT}$ was substantial at both the shoulder and elbow, even for joint DOFs directly influenced by gravity. For the shoulder, absolute $M_{INT}$ impulses and work were up to 19

and 40% of the total in the *Y* and *X* directions, respectively. Absolute $M_{INT}$ impulses were up to 28% of the total impulse and work for the elbow. $M_{SEG}$, in contrast, was a small component of the total joint moments during both reach and retrieval (Fig. 5). Absolute $M_{SEG}$ impulses and total work for the elbow did not exceed 9%. For the shoulder, $M_{SEG}$ impulses or work did not exceed 11% of the total in any direction.

Shoulder and elbow moments were linearly related

During both reach and retrieval, resultant moments between the shoulder and elbow were linearly related (Fig. 6a, b). Shoulder and elbow resultant moments were correlated with $\Phi_{LM}$ values greater than 0.91 (Table 2). This was due to strong a correlation ($\Phi_{LM} > 0.89$) among the moment components $M_{GRAV}$, $M_{INT}$, and $M_{SEG}$ at the shoulder and elbow.

Reciprocal movements could be described as minor modifications of lumped-parameter model values

For a substantial part of both reach and retrieval, $M_{GM}$ for the joint DOFs primarily affected by gravity were linearly related to joint angle (Fig. 6c, d). During the transition from reach to retrieval, there was a discontinuity, as continued shoulder abduction and elbow extension were coupled with decreasing moments. This transient period was associated with inflections in interaction moments for both the shoulder and elbow, switching from augmenting to opposing the gravitational moments (Figs. 3c, g, 5e, f). These interaction moment transients, however, were of

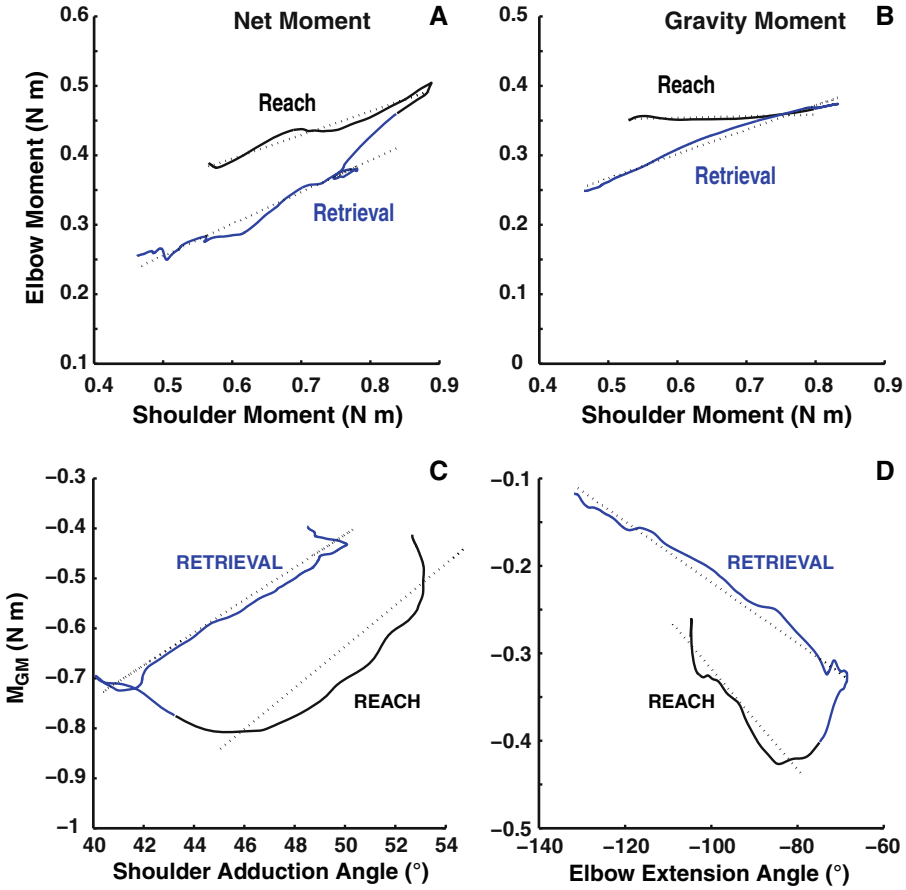


**Fig. 6** Joint moment relationships. Data from all trials were normalized in time to the mean duration of reach and retrieval phases of motion across all trials. Resulting normalized time series were averaged for each monkey as in Fig. 2, and then averaged across monkeys (*solid lines*). *Dotted lines* represent least-squares linear fits to averaged data, similar to the fits performed for individual trials and used to calculate the parameters *k* and *b*. **a** Generalized muscle moment, $M_{GM}$ ($M_{GM,S} = 0.34M_{GM,E} + 0.19$; $r^2 = 0.97$ for reach; $M_{GM} = 0.46M_{GM,E} + 0.03$; $r^2 = 0.95$ for retrieval). **b** Moment due to gravity, $M_{GRAV}$ ($M_{GRAV,S} = 0.02M_{GRAV,E} + 0.34$; $r^2 = 0.30$ for reach; $M_{GRAV,S} = 0.35M_{GRAV,E} + 0.09$; $r^2 = 0.98$ for retrieval) for elbow versus shoulder. **c**, **d** Relationship between $M_{GM}$ and angle ($\theta$) for shoulder adduction ($M_{GM} = 0.04\theta - 2.70$; $r^2 = 0.79$ for reach; $M_{GM} = 0.03\theta - 2.06$; $r^2 = 0.95$ for retrieval) and elbow extension ($M_{GM} = 0.003\theta - 0.57$; $r^2 = 0.96$ for reach; $M_{GM} = 0.006\theta - 0.89$; $r^2 = 0.87$ for retrieval)

**Table 2** Mean linear merit values for individual food retrieval trials

| | Reach | Retrieval |
|---|---|---|
| Net (Muscle) moment | 0.91 ± 0.08 | 0.93 ± 0.04 |
| Gravity moment | 0.92 ± 0.08 | 0.99 ± 0.01 |
| No gravity moment | 0.91 ± 0.07 | 0.93 ± 0.04 |
| Interaction moment | 0.95 ± 0.02 | 0.94 ± 0.03 |
| Segment moment | 0.89 ± 0.11 | 0.92 ± 0.03 |

short duration, and even with these transients average $\Phi_{LM}$ values for individual trial linear fits of moment to angle for shoulder abduction were 0.88 ± 0.03 during reach and 0.95 ± 0.05 during retrieval. For the elbow, $\Phi_{LM}$ values were 0.91 ± 0.07 for reach and 0.99 ± 0.01 for retrieval.

The linear relationship between moment and angle suggests that moment production can be described by a linear spring-like function, $M_{GM} = k\theta + b$. Although this type of lumped-parameter relationship can be useful for describing the overall mechanical function of joints or limbs, it is important to emphasize that it does not imply that joints act as classical springs (Latash and Zatsiorsky 1993). Although muscles and tendons can store and return energy in a spring-like manner, these properties are unlikely to describe joint or limb behavior over the full range of movement (Rack and Westbury 1974). The slope $k$, therefore, represents "quasi-stiffness", and the intercept $b$, represents an offset analogous to the "rest length" of a spring, but more specifically a level of tonic moment. The quasi-stiffness, $k$, for shoulder adduction during reach was not significantly different from its value during retrieval (0.59 ± 1.14 vs. 0.80 ± 0.82 N m rad$^{-1}$; $P = 0.67$), and neither were significantly different from zero. For elbow flexion/extension, $k$ was significantly higher during reach than retrieval (−0.38 ± 0.22 vs. −0.21 ± 0.14 N m rad$^{-1}$; $P = 0.02$). Measured shoulder $k$ was variable, primarily due to one monkey (26967) that used very small shoulder movements during the task (Fig. 4a), substantially increasing the mean variance in shoulder excursion across all monkeys. Removing this monkey and calculating $k$ for the remaining 4 monkeys changed the measured values, but did not result in significant differences (1.02 ± 0.71 vs. 1.14 ± 0.36 N m rad$^{-1}$; $P = 0.99$). Shoulder and elbow $b$ magnitudes were significantly higher during reach than during retrieval (shoulder: −0.80 ± 0.13 vs. −0.62 ± 0.04 N m rad$^{-1}$; $P < 0.0001$; elbow: −0.47 ± 0.15 vs. −0.30 ± 0.09 N m rad$^{-1}$; $P = 0.0001$). Excluding monkey 26967 did not appreciably affect either the mean values or the statistical comparisons.

Muscle activity during the reach and retrieval phases of movement also was consistent with the regulation of joint mechanical behavior as suggested by the lumped-parameter model. During both the reach and retrieval phases of movement, the elbow exhibited a flexor $M_{GM}$ and the shoulder generated abductor $M_{GM}$. Despite variability in the muscle activity patterns used to generate reaching and retrieval movements, a shoulder adductor and elbow extensor, triceps, was activated prior to and during reach, and during the early part of retrieval for some monkeys (Fig. 7). Triceps activity during reach for three of the four monkeys with EMG implants was consistent: between 42 and 48% of that during retrieval, with reach activity in monkey 26967 being 124% of retrieval activity. The activity of the triceps concurrent with abductor and flexor $M_{GM}$ suggests a co-activation strategy about the shoulder and elbow similar to that observed in the forearm and hand. The finger extensor (EDC) was co-activated with the finger flexor (FDS) and the thumb flexor (pollicis) during reach. FDS activity diminished during retrieval. Despite elbow flexor moments, biceps activity did not closely parallel elbow $M_{GM}$. Elbow $M_{GM}$ impulses during retrieval were 2.3-fold greater than during reach, whereas integrated biceps EMG was over 8-fold greater during retrieval.

## Discussion

Unconstrained, three-dimensional reaching behavior was consistent with a dynamic prehension strategy in which movements emerged from the interaction of both muscle and interaction joint moments with gravity. The joint behavior associated with movement could be described using the mechanical analogs of springs, with reach and retrieval associated with minor modifications of quasi-stiffness parameters.

In the reach and food retrieval task studied, the monkeys did not select straight endpoint paths. The variability and curved trajectories contrast with the more linear and consistent parasagittal-plane movements made by humans (Soechting and Lacquaniti 1981; Lacquaniti and Soechting 1982). During the reach phase of movement, $r_{max}$ was 1.6 times the forearm length. The relatively small flexion/extension and abduction movements at the shoulder resulted in the endpoint paths being dominated by elbow movement and humeral rotation, and consequently were curved (Fig. 2; Table 1). Movement curvature may reflect the unconstrained nature of the selected tasks, as humans also have been reported to use more curved paths during unconstrained movements (Atkeson and Hollerbach 1985; Desmurget et al. 1997), and monkeys show curvature during similar reaching tasks (Wenger et al. 1999). In addition, monkeys also show curvature during more constrained center-out tasks (Scott et al. 1997).

Previous studies of human arm movements have discounted the influence of gravity relative to segment interactions (Hollerbach and Flash 1982). However, the unconstrained three-dimensional reaching movements by

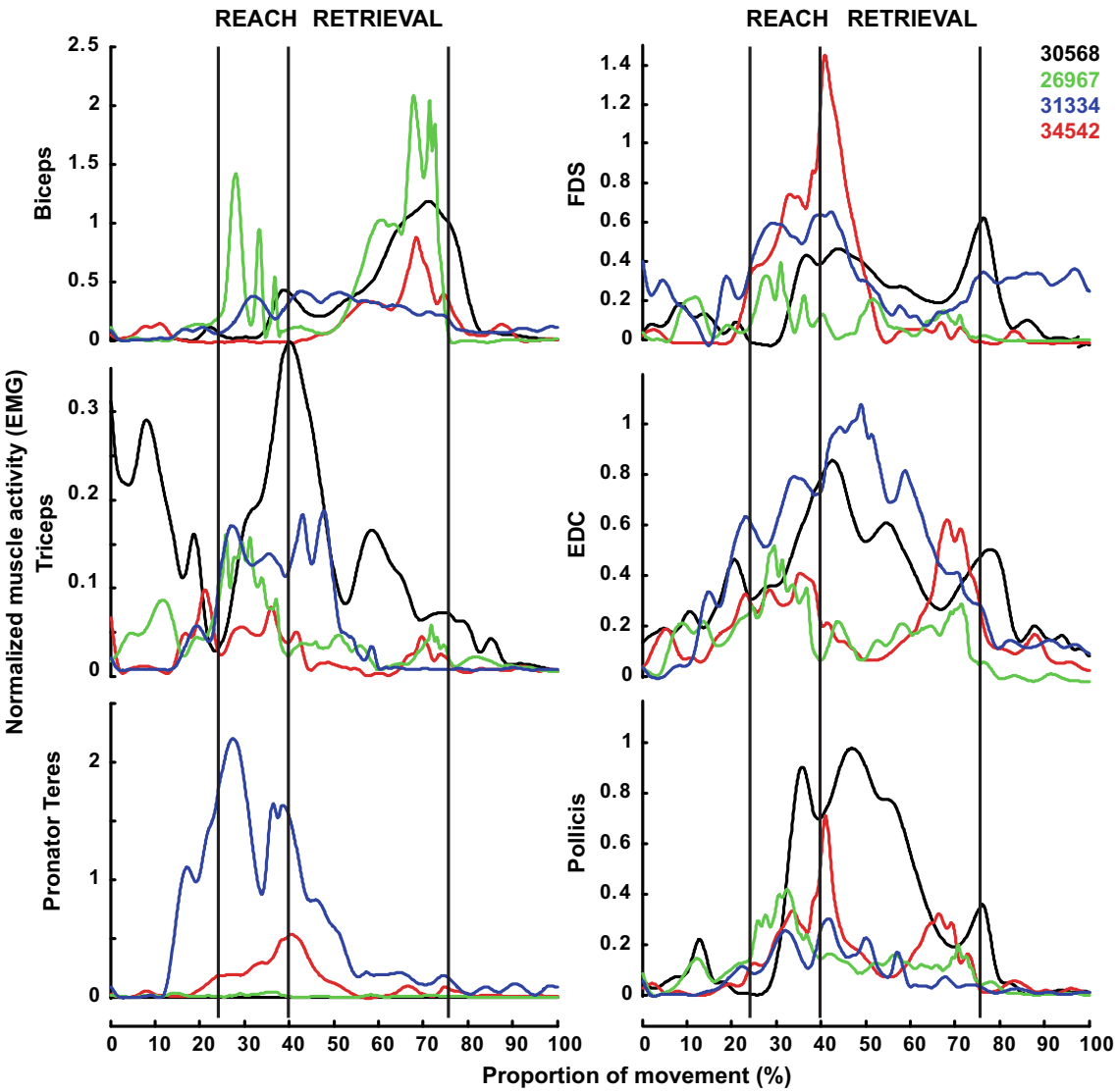


**Fig. 7** Muscle activity for arm muscles during unconstrained, three-dimensional reach and retrieval tasks. Raw EMG activity was filtered, rectified, and normalized to peak EMG activity during locomotion at 0.45 m $s^{-1}$. Data from all trials were normalized in time to the mean duration of the reach and retrieval phases of motion across all trials. Data from 1 s before reach and 1 s following retrieval are also displayed. Resulting normalized time series then were averaged for each monkey

Rhesus monkeys were dominated by gravity. $M_{SEG}$ and $M_{INT}$ were less than half of $M_{GRAV}$ (in all but shoulder $Z$ which was un-coupled from gravity). The balance of interaction and muscle moments with gravity appeared to organize joint behavior. For example at the elbow, during reach $M_{INT}$ was in the same direction as $M_{GRAV}$, and summed to overcome flexor $M_{GM}$ and cause extension. During retrieval, $M_{INT}$ opposed gravity, resulting in elbow flexion despite decreased $M_{GM}$.

Monkeys and humans appear to use comparable kinematic strategies for object retrieval (Roy et al. 2000, 2002, 2006; Mason et al. 2004). Morphological differences, however, could change the magnitude of $M_{GRAV}$ for monkeys and humans. To investigate this possibility, we calculated the joint moments using movement kinematics measured from the monkeys, but using morphological and inertial properties calculated for a hypothetical 74 kg human male, as reported in the literature (de Leva 1996). Human arm segments are 4-fold as massive with 10-fold greater moment of inertias compared to monkey arm segments. Based on these calculations, joint moments estimated for humans remain dominated by gravity. Moments due to gravity estimated for humans would account for 55–86% of the total absolute impulses, and 45–78% of the total absolute works for the human shoulder and elbow DOFs (compare to Fig. 5). In contrast, interaction moments would account for 11–45% of the impulses, and 18–54% of the work in humans.

Although it appears that gravity could be an important determinant of movement for both monkeys and humans, monkeys have been shown to use greater elbow movements and smaller shoulder movements than humans during seated food retrieval (Christel and Billard 2002). The elbow excursions of 77 ± 11° that the monkeys used for the present task were comparable to the 81 ± 20° excursions reported by Christel and Billard (2002). The greater shoulder movements used by humans could potentially result in a greater role of interaction moments relative to gravitational moments.

Monkeys showed a linear coupling of shoulder and elbow joint moments similar to that observed in humans (Gottlieb et al. 1996b; Thomas et al. 2005). One question is whether the linear dynamic coupling between the shoulder and elbow joint moments reflects an organizing control principle or a biomechanical constraint. Decomposing joint moments into components suggests that a substantial portion of the linear coupling of $M_{GM}$ between the shoulder and elbow joints emerges from passive mechanical factors. A majority of the $M_{GM}$ acted to resist gravity. Shoulder and elbow $M_{GRAV}$ were tightly coupled, with $\Phi_{LM}$ values of 0.92 and 0.99 for reach and retrieval, respectively. To a large extent, this coupling reflects direct transfer of forces due to gravity in segmented systems. Moments due to gravity at a joint are the sum of moments due to the weight of the immediately distal segment and the forces and moments at the distal joint transformed into the proximal coordinate frame (see "Appendix", Eqs. 24, 25). Consequently, when the forearm orientation is not close to vertical, a substantial amount of shoulder moment is directly transferred from the elbow. Moments necessary to resist gravitational acceleration of the forearm will require proportional moments at the shoulder to maintain a specific posture. Because muscle moments for unconstrained, three-dimensional reaching were dominated by gravity, it is likely that propagation of $M_{GRAV}$ contributed substantially to the linear $M_{GM}$ relationships during reaching and retrieval movements. Analogous coupling among non-gravitational (e.g., interaction) moments could potentially explain coupling between shoulder and elbow moments when gravity is factored out (Gottlieb et al. 1996a).

The relationship of joint angle to moment during prehension for both the shoulder in abduction/adduction and the elbow in extension/flexion could be described using a lumped-parameter model based on the analogy that these joints act as linear torsional springs. Given an initial posture, movements during both reach and retrieval could have resulted from the interaction of joints acting in a spring-like manner and gravity (Kalveram et al. 2005).

The transition from reach to retrieval involved decreasing the "rest length" offset magnitude $b$ at the shoulder, reducing the abductor moment, and allowing gravity to initiate shoulder adduction. The interaction moments caused by this adduction then contributed to elbow flexor moments that accelerated the forearm in flexion.

Consequently, a modest shift in shoulder moment (i.e. $b$) could cause large changes in movement kinematics, i.e., produce a transition from elbow extension to flexion. The shift in $M_{INT}$ related to changing $b$ allowed for retrieval movements that were more extensive (Table 1) and involved greater amounts of total work (Fig. 5d, f) than during reaching, but required less muscle work (Fig. 5f) and lower joint quasi-stiffness at the elbow. This is consistent with studies of sagittal-plane reaching-retrieval studies in humans, where interaction moments showed opposite patterns to muscle moments (Bastian et al. 1996). A slight change in shoulder moments caused interaction moments to switch signs and contribute to muscle moments, resulting in elbow flexion during retrieval. This pattern is similar to learned movement patterns that use interaction moments to reduce required muscle moments (Marconi and Almeida 2008). These patterns are also consistent with the hypothesis that the shoulder acts as a "leading" joint that causes interaction moments to contribute to reciprocal movements (Dounskaia 2005).

The transition from reach to retrieval, therefore, was achieved by taking advantage of interaction moments to change the joint moments and contribute to flexion. Triphasic $M_{SEG}$ patterns (as observed for muscle moments during human movements; (Almeida et al. 2006), emerged from unimodal $M_{GM}$ patterns (compare Fig. 3d, h to a, e). Segment motions resulted from a balance between muscle, gravitational, and interaction forces and moments. Segment movement pattern was not strongly linked to any one component. In addition, the curvature of the endpoint paths observed during these motions suggests that movement dynamics, not linear endpoint kinematics, were coordinated.

Although reach and retrieval involved nearly reciprocal movements, the muscles of the arm appeared to be co-activated throughout the trial. Although triceps activity may be necessary to accelerate the forearm during the early part of reach, triceps opposed the required $M_{GM}$ during the majority of reach and the initial period of retrieval. The interpretation of triceps activity during retrieval, however, is complicated by the fact that triceps is likely contracting eccentrically. During eccentric contractions, less activation is necessary to generate forces comparable to the concentric contractions during reach (Curtin and Edman 1994; Enoka 1996). The decrease in activity during retrieval, consequently, does not exclude the possibility that the triceps continues to produce force during this period. This pattern of co-activation is consistent with studies of discrete human

movements, which show triceps activity even during elbow flexion against gravity (Virji-Babul et al. 1994). Muscle co-activation could serve to improve the accuracy of the movements during reach and retrieval (Gribble et al. 2003; Selen et al. 2005) or to maintain joint stability (Hogan 1984). Co-activation also is clearly evident for the distal arm muscles (FDS, EDC, and pollicis), similar to the co-activation observed during precision grip tasks (Brochier et al. 2004).

We found highly variable activity in one of the primary flexors of the elbow (biceps) that could contribute to opposing gravity and to accelerating the forearm during the end of reach and during retrieval. Integrated biceps EMG activity for three of the monkeys during reach ranged from 6 to 20% of the integrated EMG during retrieval. Only one monkey (26967) showed a substantial amount (32%) of biceps activity during reach. Similar to the triceps during retrieval, during reach low levels of biceps activity do not exclude the possibility of force generation. In addition, the biceps has a complex architecture, and EMG from a single region may not accurately reflect activity of the entire muscle. Other flexor muscles, e.g., brachioradialis, from which we did not record, also may have been recruited during reach and/or retrieval, and possibly differentially recruited among monkeys. Consequently, the low levels of biceps activity observed in most monkeys during reach does not in itself allow us to reject the hypothesis that monkeys used co-activation during these movements.

In conclusion, our results support the hypothesis that by tuning shoulder and elbow mechanical properties, the interaction of the arm with gravity could result in coordinated arm movement during prehension. Interaction moments facilitate the generation of nearly reciprocal movements using relatively modest changes to joint quasi-stiffness at the reach-to-retrieval transition. Endpoint trajectories and linear coupling between the elbow and shoulder joints may be emergent properties. These relationships may be useful for evaluating motor recovery after a neuromotor injury and in the design of brain–machine neuroprosthetic systems (Courtine et al. 2007; Kim et al. 2007).

**Acknowledgments** This project is supported by grant 5R01NS042291-07 from the National Institutes of Health (NINDS). We would like to thank Ravi Gupta for helping with data analysis, and the members of the University of California, Los Angeles Neuromuscular Research Laboratory for valuable support. We thank Natalia Dounskaia and the members of the Center for Adaptive Neural Systems at Arizona State University for critically reading the manuscript.



## Appendix

The iterative Newton–Euler algorithm described by Luh et al. (1980) can be used to calculate the inverse dynamics of a serial segment mechanism (Luh et al. 1980; Craig 1989). A segment is characterized by an orientation frame, $R$, mass $m$, inertia tensor $I$, location of the link relative to the previous link $P$, and location of the link COM, $P_c$. In three dimensions, $R$ and $I$ are expressed as $3 \times 3$ matrices, $P$ and $P_c$ can be expressed as $3 \times 1$ vectors and $m$ is a scalar. The motion of the segment can be described by the $3 \times 1$ linear velocity and acceleration vectors $v$ and $\dot{v}$, and the $3 \times 1$ angular velocity and acceleration vectors, $\omega$ and $\dot{\omega}$.

Vector and matrix parameters must be expressed relative to a frame of reference. In the notation of Craig (1989), the frame of reference in which a parameter is expressed is denoted by a leading superscript. For example, the COM position of link $i$ in the reference frame $A$ would be denoted ${}^{A}P_{ci}$. Leading superscripts and subscripts are used to describe one orientation frame relative to another, i.e. identifying a rotational operator. For example, the orientation frame of link $i$ relative to the reference frame $A$ can be indicated using the notation ${}^{A}_{i}R$. Relative segment orientations and associated rotation operators can be determined by sequences of rotations about changing axes, as expressed by the Euler angles $\theta_x$, $\theta_y$, and $\theta_z$. Parameters describing the COM are further denoted using the subscript $c$, for example the linear velocity of the COM is denoted $v_c$.

The iterative Newton–Euler algorithm can be used to calculate joint moment and internal forces based on known mechanism kinematics and endpoint forces if present. The calculations are made for each sampled time point over the entire trial: the state of the arm at each time point is determined and is independent of other time points. For each link ($i$) of the mechanism, the acceleration of the COM, $\dot{v}_{c_i}$, can be calculated based on the kinematics of the previous link ($i-1$), the structure of the link, and the movements of link $i$ relative to link $i-1$. From $\dot{v}_{c_i}$, the force on the link ($F_i$) can be calculated using Newton's equation

$$F = m\dot{v}_c. \tag{2}$$

Similarly, the moment ($N_{i+1}$) acting on link $i$ can be calculated from the angular velocity and acceleration of the previous link $i-1$, the relative motion of $i$ relative to $i-1$, and the structure of the link by calculating the angular velocity and acceleration of link $i$ and using Euler's equation

$$N = {}^{c}I\dot{\omega} \times {}^{c}I\omega. \tag{3}$$

As described by Craig (1989), a set of equations allowing the calculation of forces and moments on link $i$,

given the movement of link $i-1$ and the structure of link $i$, is:

$$^{i}\omega_i = {}_{i-1}^{i}R^{i-1}\omega_{i-1} + \dot{\theta}_i \tag{4}$$

$$^{i}\dot{\omega}_i = {}_{i-1}^{i}R^{i-1}\dot{\omega}_{i-1} + {}_{i-1}^{i}R^{i-1}\omega_{i-1} \times \dot{\theta}_i + \ddot{\theta}_i \tag{5}$$

$$^{i}\dot{v}_i = {}_{i-1}^{i}R\left(^{i-1}\dot{\omega}_{i-1} \times {}^{i-1}P_i + {}^{i-1}\omega_{i-1} \times \left(^{i-1}\omega_{i-1} \times {}^{i-1}P_i\right) + {}^{i-1}\dot{v}_{i-1}\right) \tag{6}$$

$$^{i}\dot{v}_{c_i} = {}^{i}\dot{\omega}_i \times {}^{i}P_{c_i} + {}^{i}\omega_i \times \left(^{i}\omega_i \times {}^{i}P_{c_i}\right) + {}^{i}\dot{v}_i \tag{7}$$

$$^{i}F_i = m_i {}^{i}\dot{v}_{c_i} \tag{8}$$

$$^{i}N_i = {}^{c_i}I_i {}^{i}\dot{\omega}_i + {}^{i}\omega_i \times {}^{c_i}I_i {}^{i}\omega_i \tag{9}$$

Note that all vectors are expressed relative to frame $i$. These equations can be applied to each successive link of the mechanism, from the base of the mechanism to the endpoint. To incorporate the forces due to gravity, a fictive acceleration equal to gravity (g) can be added to the base of the chain:

$$^{0}\dot{v}_0 = -g. \tag{10}$$

The resulting "outward" terms $F_i$ and $N_i$ for each link represent the force and moment to resist gravity, generate segment motion, and the interactions from the more proximal segments. Similar calculations will account for forces and moments due to interaction with the more distal segments.

To calculate the "outward" components of the forces and moments necessary to resist gravity, the same iterative procedure can be used, but with the velocity and acceleration terms set to zero. In this case,

$$^{i}Fg_i = m_i {}_{i-1}^{i}R(-g). \tag{11}$$

To calculate the components of the moments due to segment accelerations, the segment angular velocity and acceleration terms can be calculated from the segment movements alone without considering the influence of the proximal joints

$$^{i}\omega s_i = \dot{\theta}_i \tag{12}$$

$$^{i}\dot{\omega}s_i = \ddot{\theta}_i \tag{13}$$

Since all the joints here are assumed to be rotational, there is no linear acceleration of the base of each segment

$$^{i}\dot{v}s_i = 0 \tag{14}$$

Consequently, the linear acceleration of the segment COM can be reduced to

$$^{i}\dot{v}s_{c_i} = \ddot{\theta}_i \times {}^{i}P_{c_i} + \dot{\theta}_i \times \left(\dot{\theta}_i \times {}^{i}P_{c_i}\right). \tag{15}$$

The segment forces and moments are therefore

$$^{i}Fs_i = m_i {}^{i}\dot{v}s_{c_i} \tag{16}$$

$$^{i}Ns_i = {}^{c_i}I_i\ddot{\theta}_i + \dot{\theta}_i \times {}^{c_i}I_i\dot{\theta}_i. \tag{17}$$

For each joint, we calculated the forces and moments, the forces to resist gravity and segment forces and moments. Forces and moments due to proximal–distal joint interactions can be calculated as

$$^{i}Fi_i = {}^{i}F_i - {}^{i}Fg_i - {}^{i}Fs_i \tag{18}$$

$$^{i}Ni_i = {}^{i}N_i - {}^{i}Ns_i \tag{19}$$

Once the forces and moments on each link caused by the proximal links have been calculated, it is possible to calculate the joint moments taking into account the influence of distal links (and if present a force ($f$) exerted on the endpoint of the arm). For each link $i$, given the distal force ($^{i+1}f_{i+1}$), it is possible to calculate the moment about the link ($^{i}n_i$) using the equations

$$^{i}f_i = {}_{i+1}^{i}R^{i+1}f_{i+1} + {}^{i}F_i \tag{20}$$

$$^{i}n_i = {}^{i}N_i + {}_{i+1}^{i}R^{i+1}n_{i+1} + P_{c_i} \times {}^{i}F_i + {}^{i}P_{i+1} \times {}_{i+1}^{i}R^{i+1}f_{i+1} \tag{21}$$

These are the "Generalized Muscle Moments," the forces and moments that must be produced actively or passively by muscles or the joint to result in the observed velocities and accelerations, considering the limb configuration at each step of time. For the forces and moments that accelerate each segment, the equations become

$$^{i}fs_i = {}^{i}Fs_i \tag{22}$$

$$^{i}ns_i = {}^{i}Ns_i + P_{c_i} \times {}^{i}Fs_i \tag{23}$$

For the forces and moments necessary to resist gravity, the equations become

$$^{i}fg_i = {}_{i+1}^{i}R^{i+1}fg_{i+1} + {}^{i}Fg_i \tag{24}$$

$$^{i}ng_i = {}_{i+1}^{i}R^{i+1}ng_{i+1} + P_{c_i} \times {}^{i}Fg_i + {}^{i}P_{i+1} \times {}_{i+1}^{i}R^{i+1}fg_{i+1}. \tag{25}$$

Finally, the interaction forces and moments, taking into account both proximal–distal and distal–proximal interactions, can be calculated as

$$^{i}fi_i = {}^{i}f_i - {}^{i}fg_i - {}^{i}fs_i = {}_{i+1}^{i}R^{i+1}fi_{i+1} + {}^{i}Fi_i \tag{26}$$

$$^{i}ni_i = {}^{i}n_i - {}^{i}ng_i - {}^{i}ns_i = {}^{i}Ni_i + {}_{i+1}^{i}R^{i+1}ni_{i+1} + P_{c_i} \times {}^{i}Fi_i + {}^{i}P_{i+1} \times {}_{i+1}^{i}R^{i+1}fi_{i+1}. \tag{27}$$

The results are forces and moments in the coordinate frame of the segment. The Euler angles used to describe segment

motion, however, were expressed in rotating reference frames beginning with the reference frame of the proximal segment. To express the moments in the coordinate frame of the corresponding joint Euler angles, they can be multiplied by the corresponding rotation operators in reverse. In the case of a *Y–Z–X* Euler angle order, the resulting moments would be

$$\tau_{xi} = \left(R_x{}^i n_i\right)\hat{X}, \tag{28}$$

$$\tau_{Zi} = \left(R_z R_x{}^i n_i\right)\hat{Z} \tag{29}$$

$$\tau_{yi} = \left(R_y R_z R_x{}^i n_i\right)\hat{Y} \tag{30}$$

where $\hat{Y}$, $\hat{Z}$ and $\hat{X}$ are the unit vectors for the *Y*-, *Z*-, and *X*-axes, respectively.

The decomposition above yields joint moments that, for each segment, satisfy the equation

$${}^i n_i = {}^i n s_i + {}^i n g_i + {}^i n i_i. \tag{31}$$

The notation of this equation can be simplified to

$$M_{\mathrm{GM}} = M_{\mathrm{SEG}} + M_{\mathrm{GRAV}} + M_{\mathrm{INT}}, \tag{32}$$

where $M_{\mathrm{GM}}$ represents generalized muscle moments, $M_{\mathrm{SEG}}$ moments reflected in segment movement, $M_{\mathrm{GRAV}}$ moments due to gravity, and $M_{\mathrm{INT}}$ interaction moments. To express these moments as an equation of motion for a given segment

$$M_{\mathrm{SEG}} - M_{\mathrm{GM}} - M_{\mathrm{GRAV}} - M_{\mathrm{INT}} = 0, \tag{33}$$

it is necessary to negate $M_{\mathrm{GRAV}}$ and $M_{\mathrm{INT}}$. These negated values are presented in the text and figures. Equation 33 can be re-arranged to Eq. 1 in the text.

Although decomposing joint moments into three orthogonal Euler angles allows for direct comparison to angles with common clinical analogs, care must be taken in interpreting these measurements. Because the limb inertial properties depend on limb configuration, joint moments about one Euler axis are likely to result in rotations in all directions (Hirashima et al. 2007a).

## References


Almeida GL, Freitas SM, Marconi NF (2006) Coupling between muscle activities and muscle torques during horizontal-planar arm movements with direction reversal. J Electromyogr Kinesiol 16:303–311

Atkeson CG, Hollerbach JM (1985) Kinematic features of unrestrained vertical arm movements. J Neurosci 5:2318–2330

Bastian AJ, Martin TA, Keating JG, Thach WT (1996) Cerebellar ataxia: abnormal control of interaction torques across multiple joints. J Neurophysiol 76:492–509

Bernstein N (1967) The co-ordination and regulation of movements. Pergamon Press, Oxford

Brochier T, Spinks RL, Umilta MA, Lemon RN (2004) Patterns of muscle activity underlying object-specific grasp by the macaque monkey. J Neurophysiol 92:1770–1782

Brock JH, Rosenzweig ES, Blesch A, Moseanko R, Havton LA, Edgerton VR, Tuszynski MH (2010) Local and remote growth factor effects after primate spinal cord injury. J Neurosci 30:9728–9737

Cheng EJ, Scott SH (2000) Morphometry of Macaca mulatta forelimb. I. Shoulder and elbow muscles and segment inertial parameters. J Morphol 245:206–224

Christel MI, Billard A (2002) Comparison between macaques' and humans' kinematics of prehension: the role of morphological differences and control mechanisms. Behav Brain Res 131:169–184

Courtine G, Roy RR, Hodgson J et al (2005a) Kinematic and EMG determinants in quadrupedal locomotion of a non-human primate (Rhesus). J Neurophysiol 93:3127–3145

Courtine G, Roy RR, Raven J et al (2005b) Performance of locomotion and foot grasping following a unilateral thoracic corticospinal tract lesion in monkeys (Macaca mulatta). Brain 128:2338–2358

Courtine G, Bunge MB, Fawcett JW et al (2007) Can experiments in nonhuman primates expedite the translation of treatments for spinal cord injury in humans? Nat Med 13:561–566

Craig J (1989) Introduction to robotics: mechanics and control. Addison-Wesley Publishing Company, Inc., Reading

Curtin NA, Edman KA (1994) Force-velocity relation for frog muscle fibres: effects of moderate fatigue and of intracellular acidification. J Physiol 475:483–494

de Leva P (1996) Adjustments to Zatsiorsky-Seluyanov's segment inertia parameters. J Biomech 29:1223–1230

Desmurget M, Jordan M, Prablanc C, Jeannerod M (1997) Constrained and unconstrained movements involve different control strategies. J Neurophysiol 77:1644–1650

Dounskaia N (2005) The internal model and the leading joint hypothesis: implications for control of multi-joint movements. Exp Brain Res 166:1–16

Dounskaia N, Wisleder D, Johnson T (2005) Influence of biomechanical factors on substructure of pointing movements. Exp Brain Res 164:505–516

Enoka RM (1996) Eccentric contractions require unique activation strategies by the nervous system. J Appl Physiol 81:2339–2346

Fisk J, Lackner JR, DiZio P (1993) Gravitoinertial force level influences arm movement control. J Neurophysiol 69:504–511

Franklin DW, Osu R, Burdet E, Kawato M, Milner TE (2003) Adaptation to stable and unstable dynamics achieved by combined impedance control and inverse dynamics model. J Neurophysiol 90:3270–3282

Galloway JC, Koshland GF (2002) General coordination of shoulder, elbow and wrist dynamics during multijoint arm movements. Exp Brain Res 142:163–180

Gentili R, Cahouet V, Papaxanthis C (2007) Motor planning of arm movements is direction-dependent in the gravity field. Neuroscience 145:20–32

Gomi H, Kawato M (1996) Equilibrium-point control hypothesis examined by measured arm stiffness during multijoint movement. Science 272:117–120

Gottlieb GL (1998) Muscle activation patterns during two types of voluntary single-joint movement. J Neurophysiol 80:1860–1867

Gottlieb GL, Corcos DM, Agarwal GC (1989) Strategies for the control of voluntary movements with one mechanical degree of freedom. Behav Brain Sci 12:189–210

Gottlieb GL, Song Q, Hong DA, Almeida GL, Corcos D (1996a) Coordinating movement at two joints: a principle of linear covariance. J Neurophysiol 75:1760–1764

Gottlieb GL, Song Q, Hong DA, Corcos DM (1996b) Coordinating two degrees of freedom during human arm movement: load and speed invariance of relative joint torques. J Neurophysiol 76:3196–3206

Gottlieb GL, Song Q, Almeida GL, Hong D, Corcos D (1997) Directional control of planar human arm movement. J Neurophysiol 78:2985–2998

Graham KM, Moore KD, Cabel DW, Gribble PL, Cisek P, Scott SH (2003) Kinematics and kinetics of multijoint reaching in nonhuman primates. J Neurophysiol 89:2667–2677

Gribble PL, Ostry DJ (1999) Compensation for interaction torques during single- and multijoint limb movement. J Neurophysiol 82:2310–2326

Gribble PL, Mullin LI, Cothros N, Mattar A (2003) A role for cocontraction in arm movement accuracy. J Neurophysiol 89:2396–2405

Hannaford B, Stark L (1985) Roles of the elements of the triphasic control signal. Exp Neurol 90:619–634

Hirashima M, Kudo K, Ohtsuki T (2007a) A new non-orthogonal decomposition method to determine effective torques for three-dimensional joint rotation. J Biomech 40:871–882

Hirashima M, Kudo K, Watarai K, Ohtsuki T (2007b) Control of 3D limb dynamics in unconstrained overarm throws of different speeds performed by skilled baseball players. J Neurophysiol 97:680–691

Hochberg LR, Serruya MD, Friehs GM et al (2006) Neuronal ensemble control of prosthetic devices by a human with tetraplegia. Nature 442:164–171

Hogan N (1984) An organizing principle for a class of voluntary movements. J Neurosci 4:2745–2754

Hollerbach JM, Flash T (1982) Dynamic interactions between limb segments during planar arm movement. Biol Cybern 44:67–77

Jackson A, Moritz CT, Mavoori J, Lucas TH, Fetz EE (2006) The Neurochip BCI: towards a neural prosthesis for upper limb function. IEEE Trans Neural Syst Rehabil Eng 14:187–190

Kalveram KT, Schinauer T, Beirle S, Richter S, Jansen-Osmann P (2005) Threading neural feedforward into a mechanical spring: how biology exploits physics in limb control. Biol Cybern 92:229–240

Kim HK, Carmena JM, Biggs SJ, Hanson TL, Nicolelis MA, Srinivasan MA (2007) The muscle activation method: an approach to impedance control of brain-machine interfaces through a musculoskeletal model of the arm. IEEE Trans Biomed Eng 54:1520–1529

Lacquaniti F, Soechting JF (1982) Coordination of arm and wrist motion during a reaching task. J Neurosci 2:399–408

Latash ML, Zatsiorsky VM (1993) Joint stiffness: myth or reality? Hum Mov Sci 12:653–692

Luh JYS, Walker MW, Paul RPC (1980) On-line computational scheme for mechanical manipulators. Trans. ASME: Journal of Dynamic Systems, Measurement, and Control 120:69–76

Marconi NF, Almeida GL (2008) Principles for learning horizontal-planar arm movements with reversal. J Electromyogr Kinesiol 18:771–779

Mason CR, Theverapperuma LS, Hendrix CM, Ebner TJ (2004) Monkey hand postural synergies during reach-to-grasp in the absence of vision of the hand and object. J Neurophysiol 91:2826–2837

Morasso P (1981) Spatial control of arm movements. Exp Brain Res 42:223–227

Nakamura T, Yabe Y, Horiuchi Y, Yamazaki N (1999) In vivo motion analysis of forearm rotation utilizing magnetic resonance imaging. Clin Biomech (Bristol, Avon) 14:315–320

Papaxanthis C, Pozzo T, McIntyre J (2005) Kinematic and dynamic processes for the control of pointing movements in humans revealed by short-term exposure to microgravity. Neuroscience 135:371–383

Pozzo T, Papaxanthis C, Stapley P, Berthoz A (1998) The sensorimotor and cognitive integration of gravity. Brain Res Brain Res Rev 28:92–101

Rack PMH, Westbury DR (1974) Short-range stiffness of active mammalian muscle and its effect on mechanical properties. J Physiol 240(2):331–350

Rosenzweig ES, Courtine G, Jindrich DL, Brock JH, Ferguson AR, Strand SC, Nout YS, Roy RR, Miller DM, Beattie MS, Havton LA, Bresnahan JC, Edgerton VR, Tuszynski MH (2010) Extensive spontaneous plasticity of corticospinal projections after primate spinal cord injury. Nat Neurosci 13(12):1505–1510

Roy AC, Paulignan Y, Farne A, Jouffrais C, Boussaoud D (2000) Hand kinematics during reaching and grasping in the macaque monkey. Behav Brain Res 117:75–82

Roy AC, Paulignan Y, Meunier M, Boussaoud D (2002) Prehension movements in the macaque monkey: effects of object size and location. J Neurophysiol 88:1491–1499

Roy AC, Paulignan Y, Meunier M, Boussaoud D (2006) Prehension movements in the macaque monkey: effects of perturbation of object size and location. Exp Brain Res 169:182–193

Sainburg RL, Ghez C, Kalakanis D (1999) Intersegmental dynamics are controlled by sequential anticipatory, error correction, and postural mechanisms. J Neurophysiol 81:1045–1056

Schaal S, Sternad D (2001) Origins and violations of the 2/3 power law in rhythmic three-dimensional arm movements. Exp Brain Res 136:60–72

Scott SH, Sergio LE, Kalaska JF (1997) Reaching movements with similar hand paths but different arm orientations. II. Activity of individual cells in dorsal premotor cortex and parietal area 5. J Neurophysiol 78:2413–2426

Selen LP, Beek PJ, van Dieen JH (2005) Can co-activation reduce kinematic variability? A simulation study. Biol Cybern 93:373–381

Shadmehr R, Mussa-Ivaldi FA (1994) Adaptive representation of dynamics during learning of a motor task. J Neurosci 14:3208–3224

Shemmell J, Johansson J, Portra V, Gottlieb GL, Thomas JS, Corcos DM (2007) Control of interjoint coordination during the swing phase of normal gait at different speeds. J Neuroeng Rehabil 4:10

Soechting JF, Lacquaniti F (1981) Invariant characteristics of a pointing movement in man. J Neurosci 1:710–720

Soechting JF, Buneo CA, Herrmann U, Flanders M (1995) Moving effortlessly in three dimensions: does Donders' law apply to arm movement? J Neurosci 15:6271–6280

Thomas JS, Corcos DM, Hasan Z (2005) Kinematic and kinetic constraints on arm, trunk, and leg segments in target-reaching movements. J Neurophysiol 93:352–364

Virji-Babul N, Cooke JD, Brown SH (1994) Effects of gravitational forces on single joint arm movements in humans. Exp Brain Res 99:338–346

Wenger KK, Musch KL, Mink JW (1999) Impaired reaching and grasping after focal inactivation of globus pallidus pars interna in the monkey. J Neurophysiol 82:2049–2060

Wu G, Siegler S, Allard P et al (2002) ISB recommendation on definitions of joint coordinate system of various joints for the reporting of human joint motion—part I: ankle, hip, and spine. International Society of Biomechanics. J Biomech 35:543–548

Wu G, van der Helm FC, Veeger HE et al (2005) ISB recommendation on definitions of joint coordinate systems of various joints for the reporting of human joint motion—Part II: shoulder, elbow, wrist and hand. J Biomech 38:981–992

Yamasaki H, Tagami Y, Fujisawa H, Hoshi F, Nagasaki H (2008) Interaction torque contributes to planar reaching at slow speed. Biomed Eng Online 7:27